G Model
JJBE-1978; No. of Pages 9

Medical Engineering & Physics xxx (2011) xxx–xxx

Contents lists available at SciVerse ScienceDirect

Medical Engineering & Physics

journal homepage: www.elsevier.com/locate/medengphy

Inverse dynamic analysis of the biomechanics of the thumb while pipetting: A case study

John Z. Wu[a,*], Erik W. Sinsel[a], Daniel S. Gloekler[a], Bryan M. Wimer[a], Kristin D. Zhao[b], Kai-Nan An[b], Frank L. Buczek[a]

[a] National Institute for Occupational Safety and Health, Morgantown, WV 26505, USA
[b] Biomechanics Laboratory, Division of Orthopedic Research, Mayo Clinic, Rochester, MN 55905, USA

ARTICLE INFO

Article history:
Received 22 February 2011
Received in revised form 25 August 2011
Accepted 15 September 2011

Keywords:
Ergonomics
Thumb
Kinematics
Joint moment
Pipette
Modeling

ABSTRACT

Thumb-push manual pipettes are commonly used tools in many medical, biological, and chemical laboratories. Epidemiological studies indicate that the use of thumb-push mechanical pipettes is associated with musculoskeletal disorders in the hand. The goal of the current study was to evaluate the kinematics and joint loading of the thumb during pipetting. The time-histories of joint angles and the interface contact force between the thumb and plunger during the pipetting action were determined experimentally, and the joint loadings and joint power in the thumb were calculated via an inverse dynamic approach. The moment, power, and energy absorption in each joint of the thumb during the extraction and dispensing actions were analyzed. The results indicate that the majority of the power is generated in the interphalangeal (IP) and carpometacarpal (CMC) joints for the pipetting action. The analysis method and results in the current study will be helpful in exploring the mechanism for musculoskeletal injuries of the hand associated with pipetting, providing a preliminary foundation for ergonomic design of the pipette.

Published by Elsevier Ltd on behalf of IPEM.

1. Introduction

Piston-driven air displacement pipettes are tools used to dispense a precise quantity of fluid in the microliter scale between containers. Although electrical pipettes are available, manual pipettes are still commonly used in biological and chemical laboratories because of their flexibility. There are basically three different designs of manual pipettes as distinguished by their operation mode: they are maneuvered by the palm, index finger, or thumb. The thumb-push pipette is the most commonly used model in laboratories. Epidemiological studies [1,2] indicate that the use of pipettes is strongly associated with musculoskeletal disorders (MSDs) in the hand and shoulder. David and Buckle [2] showed that almost 90% of pipette users, who continuously used the pipettes for more than an hour on a daily basis, reported hand and/or elbow disorders. Pipetting operation often requires the operators to hold their arm away from their body, necessitating static muscle forces in the shoulder girdle. In addition, the precision tasks and spacial dimensions of the workplace often necessitate flexion and/or rotation of the neck for prolonged time periods. Consequently, some pipette users complain of discomfort not only in the thumb, wrist, and elbow [3,4], but also in the shoulder and neck [2,5]. All these results are based on epidemiological studies; the mechanism of pipetting-related MSDs in the hand has not been explored previously.

From a biomechanical point-of-view, pipetting associated MSDs in the hand are likely a consequence of excessive loading conditions in the musculoskeletal system. Few researchers have quantified the force applied on the pipette and musculoskeletal loading while pipetting. Fredriksson [6] assessed the push forces at the thumb required to operate a pipette and compared them with the participants' thumb strength. She found that the peak push force in operating the pipette is 18.4% and 14.5% of the push force capacity for female and male subjects, respectively. More biomechanical analysis was performed by Asundi et al. [7] to evaluate the thumb push force and muscle activity for different pipetting tasks. They found that high-precision tasks significantly increased static muscle activity but reduced peak thumb force on average 5% as compared with low-precision tasks; in addition, pipetting high-viscosity fluids increased peak thumb forces on average 11% as compared with pipetting low-viscosity fluids.

Clinical observations indicate that the thumb is one of the most vulnerable parts of the hand for injuries in sports [8,9]. Acute injuries of the ulnar collateral ligament of the metacarpophalangeal (MP) joint of the thumb are common in sports-related thumb injuries [10,11]. MP joint injuries are likely associated with excessive joint loading during impact forces in sports. Although the

* Corresponding author at: NIOSH/CDC, 1095 Willowdale Road, MS-2027, Morgantown, WV 26505, USA. Tel.: +1 304 285 5832; fax: +1 304 285 6265.
E-mail address: jwu@cdc.gov (J.Z. Wu).

1350-4533/$ – see front matter. Published by Elsevier Ltd on behalf of IPEM.
doi:10.1016/j.medengphy.2011.09.012

magnitude of the impact forces that the thumb may experience in occupational activities will not be as great as that in sports, the duration of loading on thumb for occupational activities is much longer. Previous studies indicated that certain occupational activities are associated with osteoarthritis in the carpometacarpal (CMC) joint of the thumb [12]. The compression force at the plunger button during pipetting reaches the magnitudes observed in other activities, such as pinching [13] and jar opening [14]. Considering the repetitive nature of the pipetting action, the thumb joints during pipetting may experience excessive loading compared to those in other activities. Despite the strong evidence that operation of the thumb-push manual pipette is related to MSDs in the thumb [2], the biomechanics of the thumb (i.e.,the kinematics, joint loading, and energy consumption in the thumb joints) during pipetting have not been quantified. It is not known if operation of the thumb-push pipette would induce excessive joint torque in the CMC joint, a factor that may potentially cause degeneration of the articulation [15].

The purpose of the current study was to characterize the kinematics, loading, and energy consumption in the joints of the thumb during pipetting. Our hypothesis is that maximal joint moment and energy consumption during pipetting occur in the CMC joint of the thumb. The study was conducted via an inverse dynamic approach.

2. Methods

2.1. Experimental set-up

A typical thumb-activated pipette (P300, Pipetman, Gilson, Inc, Middleton, WI, USA) was used in the study (Fig. 1A). This type of pipette is actuated by a thumb-push button to extract and to dispense fluid, whereas there is a separate button to eject the disposable tip. The plunger can be depressed fully in two stages – for a displacement of 12 mm up to the first stop and 6 mm further to the second stop – for a total travel distance of 18 mm. The stiffness of the spring mechanism for the first stage (displacement 0–12 mm) is much smaller than that for the second stage (displacement 12–18 mm). In a typical task, the operators first press the plunger to the first stop, extract the sample fluid from the container by releasing the plunger, point the tip to a second container, and dispense the fluid by depressing the plunger to the second stop. The operators will then press the tip release button to eject the disposable tip after finishing the task. Since the tip release button is less frequently used and requires less push force, we focused only on the plunger action in this study.

In order to measure the plunger press force, we placed a film force sensor (Type C500, Pressure Profile Systems, Inc., Los Angeles, CA) on the top of the plunger button (Fig. 1C). The measurement precision (repeatability) of the system has been tested to be less than 0.1 N. To minimize the effects of the force time-drift, we preheated the instrument for at least 20 min before data collection. We have estimated the force time-drift by starting the data collection without applying force, and subtracted the force drift from the collected data in the data processing. In order to eliminate the nonlinearity of the force sensor, we calibrated the force sensor in a range of 0–50 N to obtain the force–voltage curve, which was used for the force measures. The relative displacement of the plunger button was measured via two motion markers placed on the plunger press button and the pipette handle (Fig. 1A).

2.2. Determination of kinematics

Kinematics for the fingers, hand, and forearm were determined using methods previously described [16,17]. Briefly, retroreflective markers (4 mm diameter hemispheres) were applied

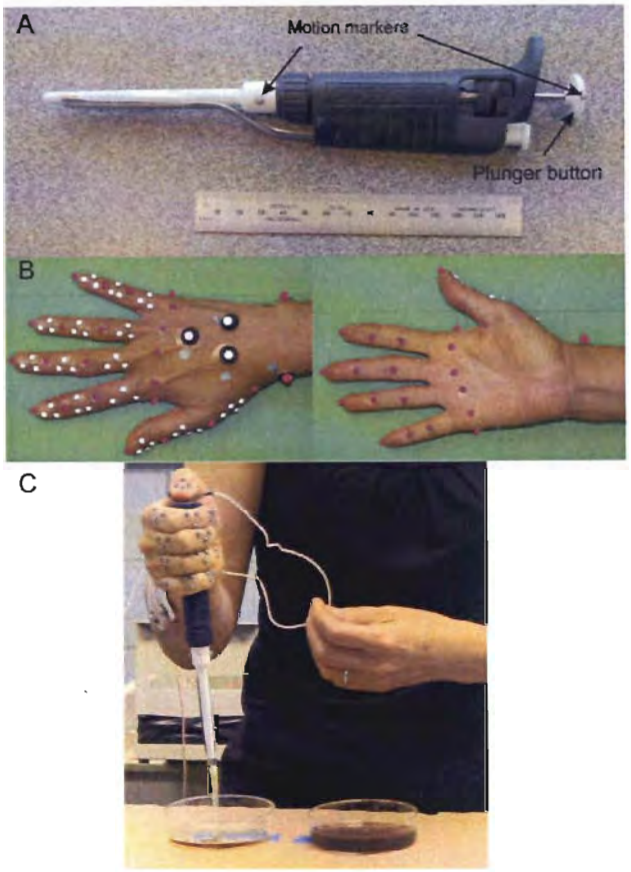

Fig. 1. Experimental set-up. (A) The pipette used in the study. (B) Calibration markers (red) and motion markers (white) placed on the subject's hand. (C) The subject operating the pipette during the testing. (For interpretation of the references to color in this figure legend, the reader is referred to the web version of the article.)

individually on the finger/thumb/hand segments using a thin self-adhesive tape (Fig. 1B). For each of the four fingers, dorsal and palmar calibration markers identified distal-interphalangeal, proximal-interphalangeal, and metacarpophalangeal joint lines, and one calibration marker identified the most distal aspect of the distal phalanx; three separate tracking markers were applied to the dorsal surface of the distal, intermediate, and proximal phalanges. For the hand segment (i.e., the aggregate of the second through the fifth metacarpals), calibration markers were applied to the medial and lateral aspect of the fifth and second metacarpal heads, respectively, and to the radial and ulnar styloids; three separate tracking markers were applied to the dorsal aspect of the hand. For the forearm segment, calibration markers were applied to the medial and lateral humeral epicondyles; a separate cluster of four least-squares tracking markers was applied via a thermoplastic shell. New for this study, dorsal and palmar calibration markers identified interphalangeal (IP) and metacarpophalangeal (MP) joint lines for the thumb, one dorsal calibration marker identified the approximate location for the carpometacarpal (CMC) joint, and one marker identified the distal aspect of the distal phalange; four separate least-squares tracking markers were applied to the dorsal surface of the distal and proximal phalanges, and the first metacarpal. Calibration markers were removed prior to pipetting tasks. The locations of the calibration markers (red) and tracking markers (white) on the subject's hand are illustrated in Fig. 1B. The measurement model consists of 12 finger segments (three segments for each of the four fingers), three thumb segments, a hand, and a forearm, with a total of 55 tracking markers used to obtain pipetting kinematics. Once

Please cite this article in press as: Wu JZ, et al. Inverse dynamic analysis of the biomechanics of the thumb while pipetting: A case study. Med Eng Phys (2011), doi:10.1016/j.medengphy.2011.09.012

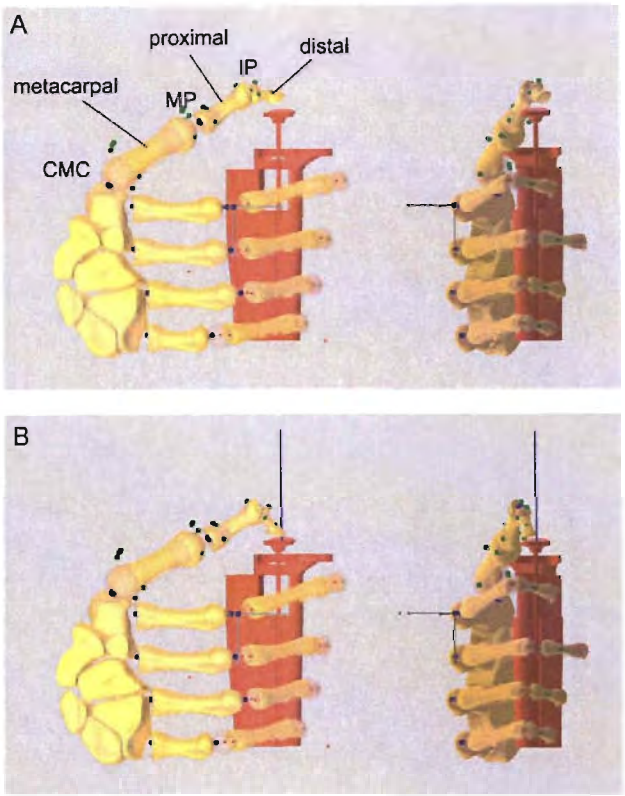

Fig. 2. The model of pipetting. (A) Released position and (B) depressed position.

the motion markers were placed on the subject's hand, they were not removed until all test sessions were completed. A 14-camera Vicon Nexus system (Oxford Metrics Ltd., Oxford, England) provided marker trajectories at 100 Hz, with calibration residuals less than 0.5 mm for a control volume approximately 3 m (wide) × 3 m (long) × 2 m (high).

2.3. Multi-body dynamic model of pipetting

The hand is modeled as a multi-body linkage system and includes four fingers (index, long, ring, and little finger), thumb, and a palm segment (Fig. 2). Each of the fingers is comprised of a distal, an intermediate, and a proximal phalanx and a metacarpal. The thumb is comprised of a distal and a proximal phalanx, a metacarpal bone, and a trapezium. The metacarpals of the four fingers and the trapezium of the thumb articulate with the palm segment. Consequently, the palm segment includes scaphoid, lunate, triquetrum, pisiform, hamate, capitate, trapezoid, trapezium, and four finger metacarpals. The mass and the principal mass moment of inertia of finger segments were adopted from a previous study [18]. The mass and the principal mass moment of inertia of the thumb segments used in the model are listed in Table 1. The segment mass and the principal mass moment of inertia were calculated using an approach by previous studies [19,18]. In the calculations, the finger and thumb segments were approximated by cylindrical bodies with ellipsoidal cross sections. The external dimensions and the bony sizes of the thumb and finger segments were based on published data [20–22]. The relative density of the soft tissues and bone were assumed to be 1.0 and 1.9 [23], respectively.

Table 1
Mass and the principal mass inertial moments of the thumb segments used in the modeling. The reference coordinate ($x - y - z$) of the mass moment of inertia was at the mass center of each segment.

Thumb segments	Mass moment of inertia (kg m^2)			Mass (kg)
	Ix	*Iy*	*Iz*	
Distal	2.201E−07	6.121E−07	5.612E−07	0.0072
Proximal	4.137E−07	1.425E−06	1.388E−06	0.0118
Metacarpal	1.106E−06	3.989E−06	4.032E−06	0.0208

The four bones of each finger were connected by three joints: distal interphalangeal (DIP), proximal interphalangeal (PIP), and metacarpophalangeal (MCP). The DIP and PIP joints were considered as hinges with one degree of freedom (DOF), whereas the MCP joint was modeled as a universal joint with two DOFs. The four bony sections of the thumb are linked via IP, MP, and CMC joints. The IP joint is modeled as a hinge with one DOF, while the MP and CMC joints are modeled as spherical joints with three DOFs. In the DIP and PIP joints of four fingers and IP joint of thumb, only the flexion/extension motion was simulated. In the MCP joints of the four fingers, the adduction/abduction and flexion/extension motions were considered. The 3-DOF joints, MP and CMC of thumb, are the most sophisticated technically and they were used to simulate the motions of flexion/extension, adduction/abduction, and internal/external rotation.

The hand model was developed on the platform of the commercial software package AnyBody (version 4.0; AnyBody Technology, Aalborg, Denmark) (Fig. 2). The model was written in Anyscript code, a programing language running on the AnyBody modeling system platform. The 3D bony meshes were obtained from CT scanning of plastic cadaveric specimens and the 3D mesh of the pipette was created using SolidWorks (Dassault Systemes SolidWorks Corp., MA, USA). The lengths of each bone mesh were scaled to fit the required phalanx lengths in the model.

2.4. Test protocol and calculation procedure

One female participant was recruited in the study. The subject is a laboratory researcher who uses manual pipettes (the model used in this study) on a daily basis. She is right-handed and has more than 10 years of experience using pipettes. The subject was instructed to pipette in postures used during routine use of pipettes. The pipette was tilted about 10 toward her right side, but the tilt angle was not requested or constrained. The workbench was adjusted to a height similar to that in the laboratory environment. The subject was instructed to extract the fluid from one container on her left side and dispense it to another container on her right side. Both containers were made of transparent plexiglass and were identical in dimension; they had a diameter of 90 mm and a height of 24 mm. The containers were placed 120 mm apart center-to-center, which was typical in her work environment. The centers of the containers were marked and clearly visible to the subject. Tap water stained light brown using regular coffee was used as the pipetting fluid in the tests. The test protocol was approved by the NIOSH Human Subjects Review Board.

The subject was instructed to repeat the same procedure in the pipetting task: (1) press the plunger button to the first stop; (2) point the pipette tip to the container center on the left side and extract the fluid from the container by releasing the button; (3) move the pipette to the second container on her right side and point the tip toward the container center; and (4) depress the plunger button all way to the second stop to completely dispense the fluid. The subject was instructed to repeat the pipetting procedure 14 times in one session. No particular pipetting rate was set for the subject. The subject was instructed to perform as she routinely does in her job. Before the data collection, the subject had a chance to practice and become comfortable with the setup for about 2 min.

Calculations were performed using an inverse dynamic approach, in which the time-histories of each joint angle and the interface contact force between the thumb tip and the pipette's

Please cite this article in press as: Wu JZ, et al. Inverse dynamic analysis of the biomechanics of the thumb while pipetting: A case study. Med Eng Phys (2011), doi:10.1016/j.medengphy.2011.09.012

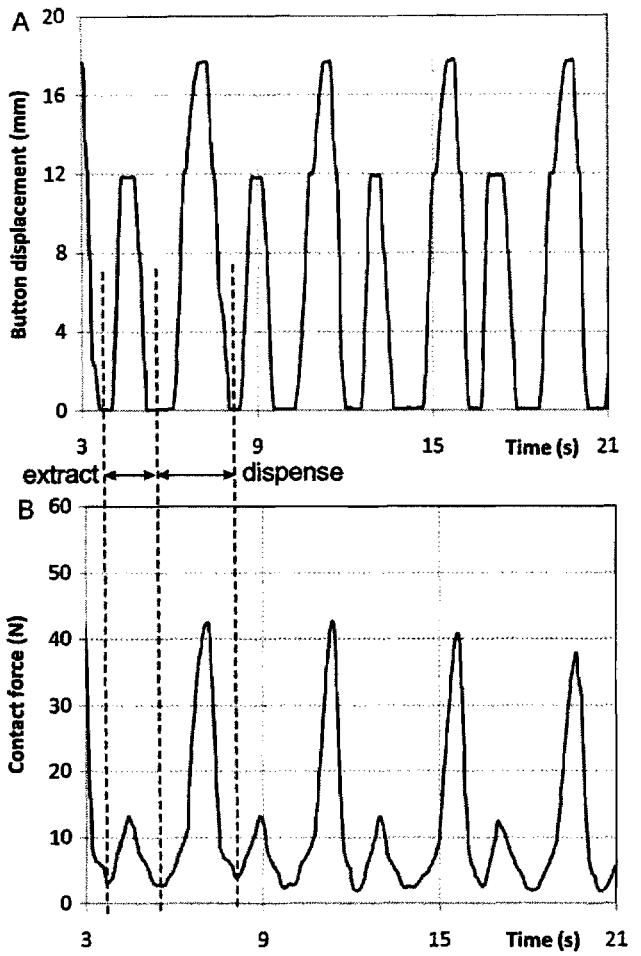

Fig. 3. Representative time-histories of the displacement and force measured at the plunger button of the pipette. (A) Button displacement and (B) button push force. The two neighboring peaks in the time-histories of the button displacement and push force represent the extraction and dispensing actions.

dispense plunger button were measured, and the corresponding time-histories of the moments and power in each joint of the thumb were calculated. The model includes the entire hand, which contains four fingers and thumb. However, we analyzed only the biomechanics of the thumb because it is the focus of this study.

3. Results

Representative time histories of the displacement and push force of the plunger button are shown in Fig. 3A and B, respectively. If we consider a cycle as the time period from the start of extraction to the completion of dispensing, the subject pipetted at a rate of 0.24 Hz on average ($n = 14$ cycles). The time duration for a work cycle is approximately 4.17 s, which contains an extraction period of 1.75 s and a dispensing period of 2.42 s. The pipette plunger moved a distance of 12 mm and 18 mm, respectively, for the extraction and dispensing task (Fig. 3A), whereas the peak push forces measured at the plunger button for the dispensing actions were about 2.5–3.0 times those for the extractions (Fig. 3B).

Since the extraction and dispensing actions are cyclic in nature, we have summarized all calculation results in terms of task cycle, as researchers traditionally do with gait analysis [24,25]. An entire work cycle is divided into the cycles of extraction and dispensing, as illustrated in Fig. 3. The plunger displacement and push force as a function of the task cycle is shown in Fig. 4A and B, respectively.

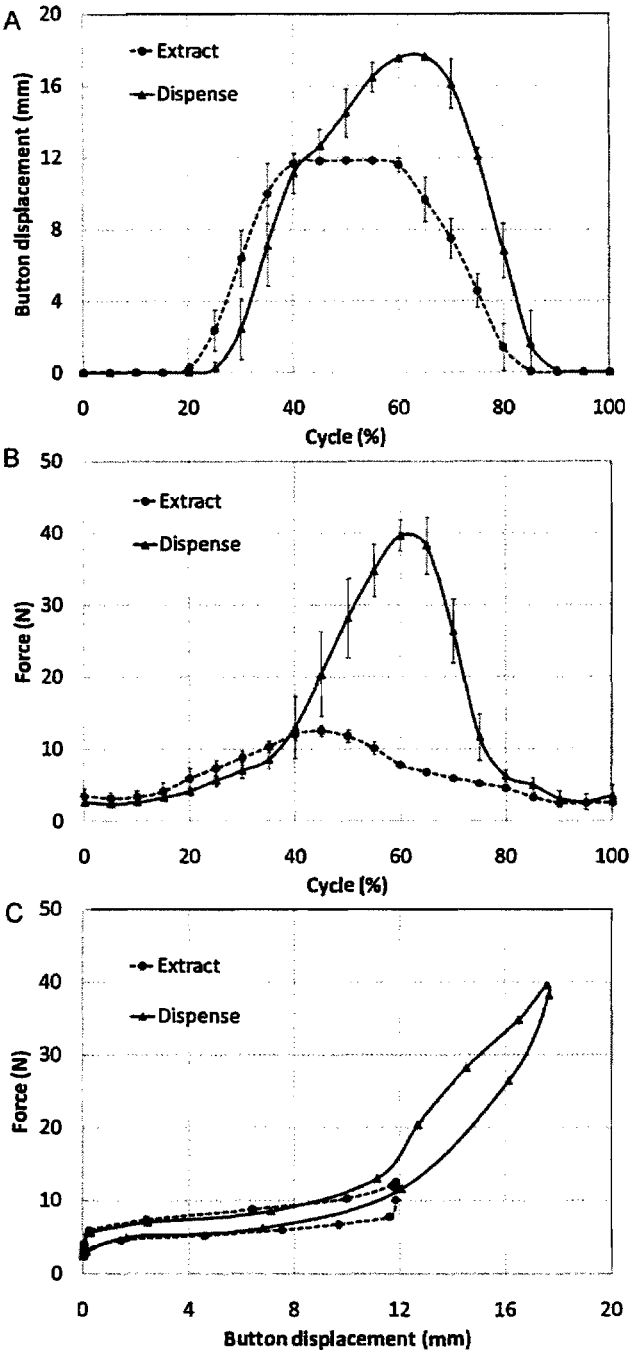

Fig. 4. Variation in the button displacement and push force during the extraction and dispensing cycles. (A) The button displacement as a function of pipetting cycle. (B) The push force as a function of pipetting cycle. (C) The push force as a function of the button displacement.

The force–displacement relationship at the plunger button during the extraction and dispensing actions, which are represented in the slope of the curves of push force versus displacement, is depicted in Fig. 4C.

There is only one DOF for the IP joint, i.e., flexion/extension motion. The IP joint angle and moment as a function of the action cycle are shown in Fig. 5A and B, respectively. The corresponding joint moment–angle relationship is shown in Fig. 5C. The joint angle for the extraction is similar to that for the dispensing action;

Please cite this article in press as: Wu JZ, et al. Inverse dynamic analysis of the biomechanics of the thumb while pipetting: A case study. Med Eng Phys (2011), doi:10.1016/j.medengphy.2011.09.012

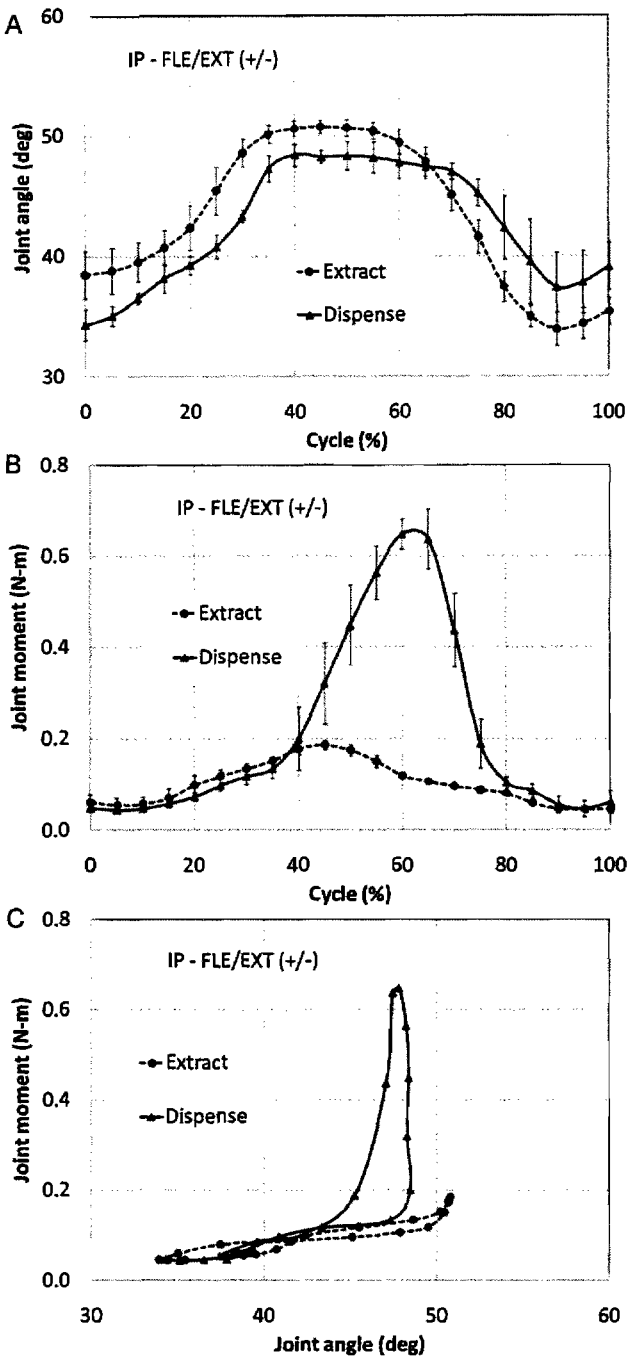

Fig. 5. Variations of the IP joint angle and joint moment during the extraction and dispensing cycles. (A) IP joint angle as a function of pipetting cycle. (B) IP joint moment as a function of pipetting cycle. (C) IP joint angle as a function of IP joint moment.

however, the peak joint moment for the dispensing action is about three times that for the extraction.

The MP joint is modeled as a spherical joint and has three DOFs. The joint angles for adduction/abduction, flexion/extension, and internal/external rotation motions as a function of the task cycle are shown in the left column of Fig. 6A–C, respectively. The corresponding joint moments for the adduction/abduction, flexion/extension, and internal/external rotation as a function of the task cycle are shown in the middle column of Fig. 6A–C, respectively. The right column of Fig. 6A–C depict the moment–angle relationship for the MP joint at the adduction/abduction, flexion/extension, and internal/external rotation motions, respectively. It is seen that the adduction/abduction and flexion/extention joint angles varied in a very small range (about 5–8°) (left column of Fig. 6A and B), whereas the internal/external rotation angle varied in a relatively larger range (8–12°) (left column of Fig. 6C) during the pipetting actions. The predominant MP joint moment is found in flexion/extension (about 2.1 N m at peak), which is approximately 5–7 times in magnitude of those observed in adduction/abduction and internal/external rotation. The peaks of the joint moments for all DOFs occurred at around 60% of the pipetting cycle.

The CMC joint is also a spherical joint and has three DOFs. The joint angles for adduction/abduction, flexion/extension, and internal/external rotation motions as a function of the task cycle are shown in the left column of Fig. 7A–C, whereas the corresponding joint moments are depicted in the middle column of Fig. 7A–C, respectively. The corresponding joint moment–angle relationship for adduction/abduction, flexion/extension, and internal/external rotation are depicted in the right column of Fig. 7A–C, respectively. The range of motion for adduction/abduction is approximately 4°; it is relatively small compared to those for the internal/external rotation and flexion/extension motions, which are in a range of approximately 12 and 15°, respectively. The peak joint moments for the adduction/abduction and flexion/extension motions reached approximately 3.0 and 2.5 N m, respectively, which are predominant compared to that for the internal/external rotation (about 0.8 N m at peak). Similar to the MP joint, the peaks of the joint moments for all DOFs occurred at around 60% of the pipetting cycle.

The power generated in the IP, MP, and CMC joints during the pipetting action is shown in Fig. 8A–C, respectively. The joint power for a single DOF is evaluated by multiplying the joint moment by the corresponding angular velocity; the power generated in a joint is considered to be the scalar summation of the power for all DOFs. Positive joint power means that the power is generated by the musculoskeletal system to perform the pipetting action, whereas negative power means that the power is absorbed in the joint. The results indicate that the majority of the power is generated in the IP and CMC joints during the pipetting action. The peak power for the extraction and dispensing action in the CMC joint reaches 0.35 and 0.61 W, respectively. The MP joint absorbs power most of the time during a working period; the peak power for the extraction and dispensing actions reaches −0.03 and −0.15 W, respectively. The peak power for the extraction and dispensing action in the IP joint reaches 0.17 and 0.51 W, respectively. The magnitude of the peak power for the dispensing action in the CMC joint is approximately 1.2 and 4.2 times of that in the IP and MP joints, respectively.

The power generated in the joints as compared with that delivered to the plunger mechanism is shown in Fig. 9. The power associated with the motion of the plunger mechanism is quantified by multiplying the contact force measured at the push button by the plunger velocity. The total joint power for the thumb is considered to be the sum of the power in all three joints [26]. A positive pushing power means that thumb musculoskeletal power is delivered to the plunger mechanism, whereas a negative value means that stored power in the plunger mechanism is returned to the thumb musculoskeletal system. It is seen that the power is positive during plunger pushing and negative during the plunger release. For both extraction and dispensing actions, the time-histories of the power cross the zero axis at approximately 65% cycle, meaning that the ratio of the period of plunger depression to release is about 1.86. During the plunger depression phase, the peak power generated in the thumb joints is 0.32 and 0.63 W for the extraction and dispensing actions, respectively; while the peak power consumed in the plunger is 0.38 and 0.43 W, respectively, for the extraction and dispensing actions. It is notable that the power generated in the joints is always greater than that consumed in

Please cite this article in press as: Wu JZ, et al. Inverse dynamic analysis of the biomechanics of the thumb while pipetting: A case study. Med Eng Phys (2011), doi:10.1016/j.medengphy.2011.09.012

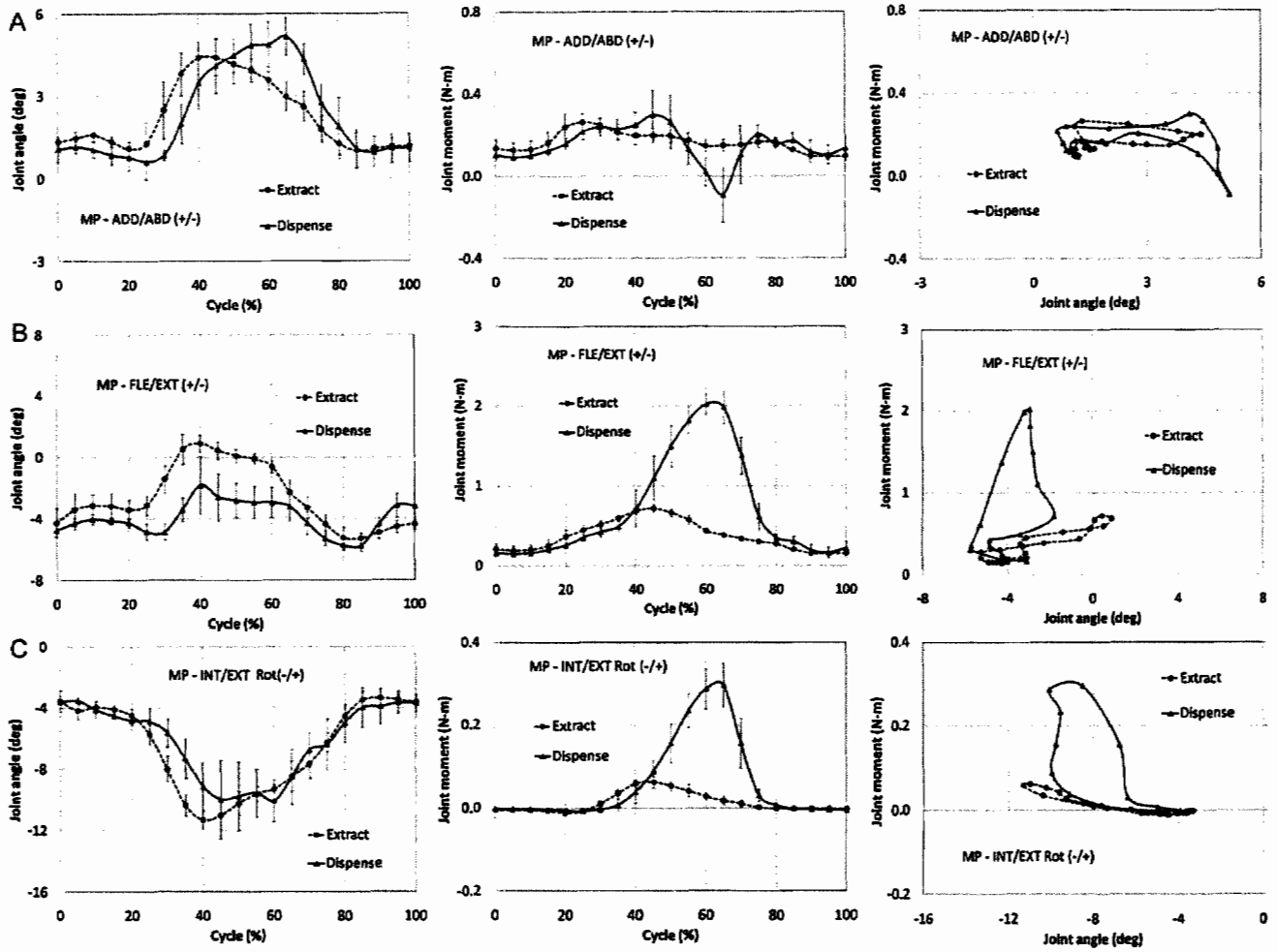

Fig. 6. Variations of MP joint angles, moment, and moment–angle relationship during a pipetting cycle. (A) MP joint motion in adduction/abduction (+/−). (B) MP joint motion in flexion/extension (+/−). (C) MP joint motion in internal/external rotation (+/−).

the plunger during the plunger depression phase (i.e., the positive power).

The energy consumption and generation during pipetting are more precisely quantified in the histories of power during the work cycle (Fig. 9). The current calculation results indicated that during approximately 56% of the pipetting cycle (Fig. 9), work is performed by the hand to push the plunger (i.e., the power is positive), while during later stage, the potential energy stored in the spring mechanism of the pipette is given back to the hand, which is characterized by the negative power. By integrating of the time-histories of the power (Fig. 9) and considering the time duration of a work cycle (extraction period 1.75 s and dispensing period 2.42 s), we calculated the energies generated in the joints and consumed in the plunger during depression, as well as the energies given back from the joints and the plunger mechanism during the release, as listed in Table 2. The energy generations and consumptions can also be calculated from the force–displacement (Fig. 7) and moment–angle relationships (Figs. 8 and 9), in which areas included in the cyclic loops represent the energy. For both extraction and dispensing actions, the power generated from the joints is about 6–7 times that consumed at the plunger mechanism. The work efficiency for the extraction and dispensing actions is evaluated to be 17.3% and 12.3%, respectively. The work efficiency is defined as the ratio of the net energy consumption by the plunger over the net energy generation from the joints. The excessive energy generated from or absorbed in the joints reflects the effort of the hand to maintain mechanical stability during the motion.

Table 2
Analysis of the energy consumption and energy generation during pipetting.

Energy	Extract			Dispense		
Consumption/ generation	Depress	Release	Net	Depress	Release	Net
Plunger (J)	0.097	−0.063	0.033	0.228	−0.172	0.056
Joint (J)	0.213	−0.022	0.191	0.596	−0.157	0.439
Efficiency (%)			17.3			12.7

4. Discussion and conclusion

The thumb-push pipette is the most common manual pipette used in university and commercial laboratories. Laboratory technicians are required to perform repetitive pipetting tasks using these devices on a daily basis and this is associated with musculoskeletal disorders in the upper limbs [3,4]. The current study represents the first biomechanical analysis of the thumb in operating a pipette. The analysis method and calculation results in the current study are useful in exploring the mechanism of musculoskeletal injuries of the hand associated with pipetting, thereby providing a preliminary foundation for ergonomic design of the pipette.

Our results showed that the maximal joint moments in the thumb occurred at approximately 60% of the cycle for the

Please cite this article in press as: Wu JZ, et al. Inverse dynamic analysis of the biomechanics of the thumb while pipetting: A case study. Med Eng Phys (2011), doi:10.1016/j.medengphy.2011.09.012

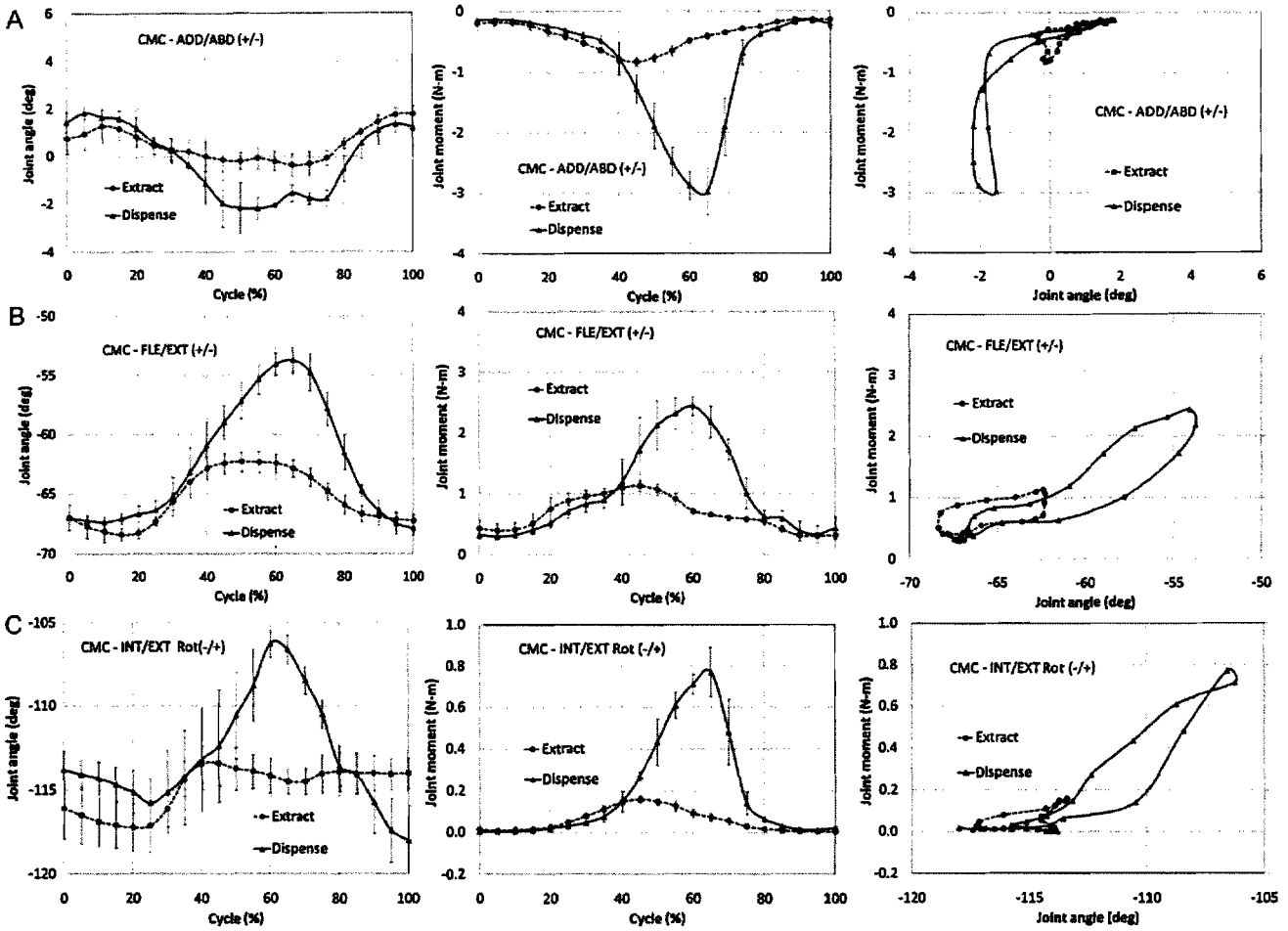

Fig. 7. Variations of CMC joint angles, moment, and moment–angle relationship during a pipetting cycle. (A) CMC joint motion in adduction/abduction (+/−). (B) CMC joint motion in flexion/extension (+/−). (C) CMC joint motion in internal/external rotation (+/−).

dispensing action (Figs. 5–7). The magnitude of the maximal moment in the CMC joint (Fig. 7) was found to reach 4.0 N m at the peak, which is approximately 1.9 and 5.7 times that in the MP (Fig. 6, 2.1 N m) and IP (Fig. 6, 0.7 N m) joints, respectively. Furthermore, the results of the energy analysis of the joints showed that the peak power generated by the joints reaches approximately 0.90 W at 50% of the cycle for the dispensing action (Fig. 9B); the power generated in the CMC joint takes about 68% the total joint power at the peak (Fig. 8C). Our results indicate that the CMC joint is loaded more than the other joints in the thumb during pipetting. This theoretical analysis is consistent with the clinical observations [12] that the CMC joint may be susceptible to developing osteoarthritis during the occupational activities, especially pipetting.

Our results show that the force–displacement curves of the pipette plunger button in loading differ from those in the unloading process, which is consistent with a previous study [7]. During the loading process, work is done by the musculoskeletal system to push the plunger, whereas the potential energy stored in the pipette spring mechanism is given back to the hand system during the unloading process. The joint power absorption during the unloading is mainly caused by the CMC joint that produces resistant flexion moment in the presence of extension; this action controls the speed of the compressed spring returning to its resting length. The area enclosed in the force–displacement loops represents the net energy consumed during the pipetting cycles.

It is widely accepted that static muscle contraction is one of the major factors that are associated with musculoskeletal disorders in occupational activities [27,28]. Using the proposed model, it would be possible to predict which muscle group in the thumb will be subjected to static loading during pipette operation. Our analysis indicated that the range of motion of the MP joint in flexion/extension varied within about 4°, whereas its corresponding peak joint moment exceeded 2 N m during the dispensing action. We would speculate from our analysis that the muscles associated with MP joint flexion/extension motion would likely be subjected to static loading during the pipetting cycle.

Since the motion markers were placed on the skin surface of the finger and thumb segments, the majority of measurement errors using the current method may come from the relative motion between skin and bony segments. Especially for the metacarpal bony segment of the thumb, the errors in kinematics may be greater than those for the other segments. This is because the metacarpal bony segment has usually a thicker soft tissue layer, which may cause larger relative motions between the bony segment and motion capture markers. In addition, the metacarpal bony segment has a relatively small range of motion during the pipetting. Consequently, a small absolute kinematics error could induce a large relative error. The uncertainty in the kinematics of the metacarpal bony segment may contribute to larger error in the joint angles of MP and CMC (Figs. 6 and 7). Alternative techniques will be sought to precisely quantify the kinematics of MP and CMC joint motions.

A limitation of the current study was that all results were derived from the tests using only a single subject. It is expected

Please cite this article in press as: Wu JZ, et al. Inverse dynamic analysis of the biomechanics of the thumb while pipetting: A case study. Med Eng Phys (2011), doi:10.1016/j.medengphy.2011.09.012

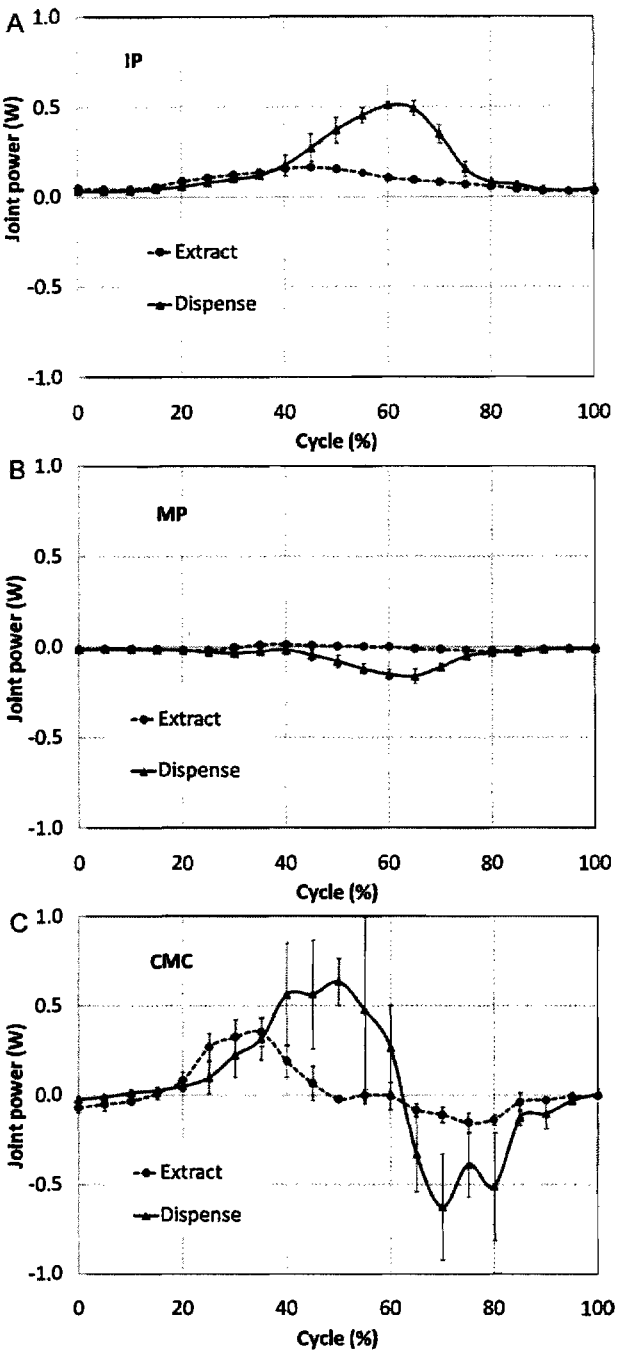

Fig. 8. Joint power as a function of the pipetting cycle. (A) IP joint. (B) MP joint. (C) CMC joint.

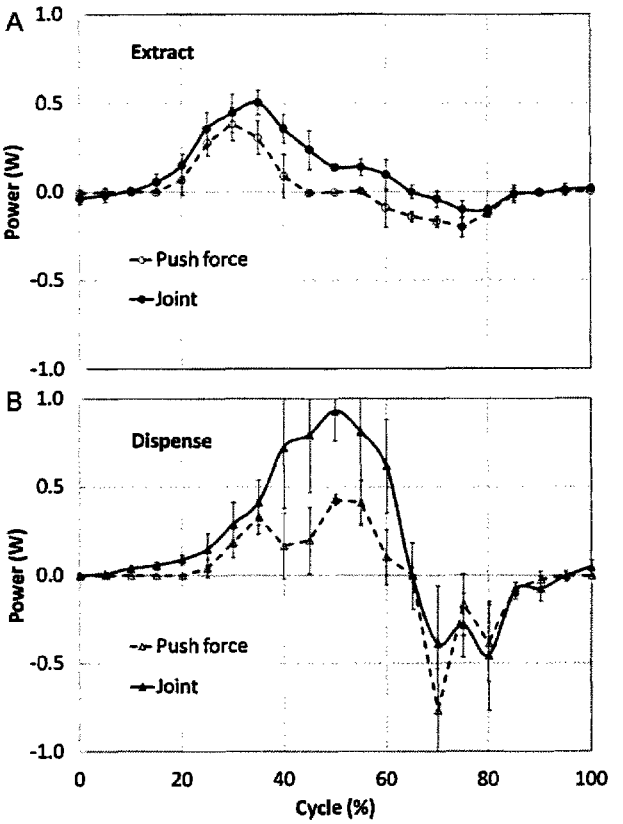

Fig. 9. Comparison of the total joint power with the power performed at the push button. (A) Extraction task. (B) Dispensing task. The joint power is the sum of the power in all three joints.

that the variability of the experimental data would be greater if more subjects were involved. Different hand sizes relative to the pipette may contribute to larger deviations in the joint motions and joint moments during pipetting. Different operators may push the pipette at different speeds, and this will result in different force–displacement curves, because the plunger mechanism of the pipette is not only non-linear but also viscous, i.e., the force–displacement curves would be different if the plunger is compressed to the same distance at different speeds. However, the maximal plunger displacement and pushing force for different subjects would likely be similar, because the maximal compression force and displacement of the pipette are dependent on the mechanism of the pipette. Therefore, the trends of the force, joint angle, joint moment, and power obtained in the study provide a preliminary foundation to understand the biomechanics of manual pipetting.

In summary, we analyzed kinematics, loading, and power generation in the joints of the thumb during pipetting. The time-histories of the joint motions, joint moments, energy generation/consumption in the joints and in the plunger of the pipette during the extraction and dispensing actions were quantified. The analysis method and results in the current study are useful in exploring the mechanism of musculoskeletal injuries of the hand associated with pipetting. However, to make recommendations on the practical pipette design, a more comprehensive study across additional subjects is needed.

Disclaimers

Mention of product and/or company name does not imply endorsement by the National Institute for Occupational Safety and Health. The findings and conclusions in this report are those of the authors and do not necessarily represent the views of the National Institute for Occupational Safety and Health.

Acknowledgements

We want to express our gratitude to Mr. Daniel E. Welcome (NIOSH), who provided technical assistance for the test set-up and constructed the digital 3D pipette model.

Conflict of interest

All authors of this manuscript have no conflict of interest.

References

[1] Bjorksten MG, Almby B, Jansson ES. Hand and shoulder ailments among laboratory technicians using modern plunger-operated pipettes. Appl Ergon 1994;25(2):88–94.
[2] David G, Buckle P. A questionnaire survey of the ergonomic problems associated with pipettes and their usage with specific reference to work-related upper limb disorders. Appl Ergon 1997;28(4):257–62.
[3] Baker P, Cooper C. Upper limb disorder due to manual pipetting. Occup Med (Lond) 1998;48(2):133–4.
[4] Heath CJ. Case report-upper limb pain attributed to repeated manual pipetting. Occup Med (Lond) 1998;48(4):279–80.
[5] McKean ML, Costello K, Scordato R, Ligugnana R. Musculoskeletal diseases caused by use of micropipette in laboratory. G Ital Med Lav Ergon 2005;27(2):240–3.
[6] Fredriksson K. Laboratory work with automatic pipettes: a study on how pipetting affects the thumb. Ergonomics 1995;38(5):1067–73.
[7] Asundi KR, Bach JM, Rempel DM. Thumb force and muscle loads are influenced by the design of a mechanical pipette and by pipetting tasks. Hum Factors 2005;47(1):67–76.
[8] Heim D. The skier's thumb. Acta Orthop Belg 1999;65(4):440–6.
[9] Morgan WJ, Slowman LS. Acute hand and wrist injuries in athletes: evaluation and management. J Am Acad Orthop Surg 2001;9(6):389–400.
[10] Baskies MA, Lee SK. Evaluation and treatment of injuries of the ulnar collateral ligament of the thumb metacarpophalangeal joint. Bull NYU Hosp Jt Dis 2009;67(1):68–74.
[11] Ritting AW, Baldwin PC, Rodner CM. Ulnar collateral ligament injury of the thumb metacarpophalangeal joint. Clin J Sport Med 2010;20(2):106–12.
[12] Winzeler S, Rosenstein BD. Occupational injury and illness of the thumb. causes and solutions. Aaohn J 1996;44(10):487–92.
[13] Chang JH, Ho KY, Su FC. Kinetic analysis of the thumb in jar-opening activity among female adults. Ergonomics 2008;51(6):843–57.
[14] Lin HT, Kuo LC, Liu HY, Wu WL, Su FC. The three-dimensional analysis of three thumb joints coordination in activities of daily living. Clin Biomech (Bristol, Avon) 2011;26(4):371–6.
[15] Feldon P, Belsky MR. Degenerative diseases of the metacarpophalangeal joints. Hand Clin 1987;3(3):429–47.
[16] Buczek FL, Sinsel EW, Gloekler DS, Wimer BM, Warren CM, Wu JZ. Kinematic performance of a six degree-of-freedom hand model (6DHand) for use in occupational biomechanics. J Biomech 2011;44(9):1805–9.
[17] Sinsel EW, Gloekler DS, Wimer BM, Warren CM, Wu JZ, Buczek FL. A novel technique quantifying phalangeal interface pressures at the hand–handle interface. In Proceedings of the 33th Annual Meeting of the American Society of Biomechanics (ASB-2010). Providence, RI, USA 2010; http://www.asbweb.org/conferences/2010/abstracts/70.pdf.
[18] Wu JZ, Dong RG, McDowell TW, Welcome DE. Modeling the finger joint moments in a hand at the maximal isometric grip: the effects of friction. Med Eng Phys 2009;31(10):1214–8.
[19] Robertson DG, Hamill J, Kamen G, Caldwell GE, Whittlesey S. Research methods in biomechanics. Human Kinetics Publishers; 2004.
[20] Garrett JW. The adult human hand: some anthropometric and biomechanical considerations. Hum Factors 1971;13(2):117–31.
[21] Buchholz B, Armstrong TJ. An ellipsoidal representation of human hand anthropometry. Hum Factors 1991;33(4):429–41.
[22] Schulter-Ellis FP, Lazar GT. Internal morphology of human phalanges. J Hand Surg [Am] 1984;9(4):490–5.
[23] Abe H, Hayashi K, Sato M. Mechanical properties of living cells, tissues, and organs. Tokyo: Springer-Verlag; 1996.
[24] Winter DA. Biomechanics and motor control of human movement. 3rd edn. Hoboken, NJ: John Wiley and Sons; 2005.
[25] Whittle MW. Gait analysis: an introduction. 4th edn. Edinburgh: Butterworth-Heinemann-Elsevier; 2007.
[26] van Ingen Schenau GJ, Cavanagh PR. Power equations in endurance sports. J Biomech 1990;23(9):865–81.
[27] Stock SR. Workplace ergonomic factors and the development of musculoskeletal disorders of the neck and upper limbs: a meta-analysis. Am J Ind Med 1991;19(1):87–107.
[28] Ranney D, Wells R, Moore A. Upper limb musculoskeletal disorders in highly repetitive industries: precise anatomical physical findings. Ergonomics 1995;38(7):1408–23.

Please cite this article in press as: Wu JZ, et al. Inverse dynamic analysis of the biomechanics of the thumb while pipetting: A case study. Med Eng Phys (2011), doi:10.1016/j.medengphy.2011.09.012